

Article

Diagnostic Analysis of Diabatic Heating in an Extreme Rainfall Event in Shandong Province, China

Yang Jiao ¹, Meng Zhang ², Yuqing Zhang ^{3,*}  and Yingjia Chu ¹¹ Jinan Meteorological Bureau, Jinan 250102, China; jiaoyang@jn.shandong.cn (Y.J.); ouccyj2009@163.com (Y.C.)² Department of Mathematics, University of Arizona, 617 N. Santa Rita Ave., Tucson, AZ 85721, USA; reneezhang@arizona.edu³ School of Geography and Planning, Huaiyin Normal University, Huai'an 223000, China

* Correspondence: 8201711019@hytc.edu.cn

Abstract: This study utilizes data from national ground meteorological observation stations in Shandong province, Fengyun-4 satellite data, and ERA5 reanalysis data. Through the calculation of atmospheric heat source changes, the role of diabatic heating in the occurrence and development of heavy rainfall is revealed. The widespread heavy-to-torrential rainfall event in Shandong province on 25 June 2018 is analyzed as a case study. It was found that a deep and robust southwest jet stream was the key system for the formation of this rainfall event. Satellite cloud images during the peak rainfall period showed vigorous development in the rainfall cloud region. During the concentrated rainfall period and when the low-altitude jet stream strengthened, there was mostly cold advection overhead at the observation station. The low-altitude jet stream transported moisture, increasing the humidity gradient, thus enhancing frontogenesis. The warm advection in the low-altitude jet stream was not the main energy supplier during heavy rainfall, and local temperature variations were the primary contributors to the thermodynamic conditions during the peak rainfall period. The rate of warming caused by the condensation and release of heat from water vapor significantly increased during the concentrated rainfall period. This warming effect played a heating role in the middle and lower layers, and the positive feedback from the latent heat release of water vapor condensation intensified the weather system affecting the rainfall, providing strong thermodynamic and dynamic conditions for heavy rainfall.

Keywords: heavy rainfall; diabatic heating; atmospheric heat source; latent heat of condensation



Citation: Jiao, Y.; Zhang, M.; Zhang, Y.; Chu, Y. Diagnostic Analysis of Diabatic Heating in an Extreme Rainfall Event in Shandong Province, China. *Atmosphere* **2024**, *15*, 66. <https://doi.org/10.3390/atmos15010066>

Academic Editors: Dae Il Jeong and Stefano Federico

Received: 24 October 2023

Revised: 24 December 2023

Accepted: 3 January 2024

Published: 5 January 2024



Copyright: © 2024 by the authors. Licensee MDPI, Basel, Switzerland. This article is an open access article distributed under the terms and conditions of the Creative Commons Attribution (CC BY) license (<https://creativecommons.org/licenses/by/4.0/>).

1. Introduction

Shandong province is located in the East Asian monsoon region, positioned at the climatic transition zone between southern and northern China. Extreme precipitation events such as heavy rainfall are relatively frequent, impacting both industrial and agricultural development [1–3]. Heavy rainfall is the result of the combined effects of multi-scale systems, among which the low-altitude jet stream plays a significant role in promoting the occurrence of heavy rainfall [4,5]. This low-altitude jet stream is a key weather system in the genesis of heavy rain, evident in its role in transporting water vapor to regions of intense precipitation. The combined action of low-altitude and high-altitude jet streams provides the necessary dynamic and thermodynamic instability conditions for heavy rainfall [6–9]. Cheng et al. [10] analyzed the continuous and widespread heavy rainfall brought to Guangdong by the strong typhoon ‘Utor’ after its landfall. It is found that the maintenance of the unstable stratification is mainly due to the warm advection to Guangdong transferred by the low-level jet. Further studies reveal a truth that the low-level jet, originally cold over the sea, is warmed and blows to Guangdong when it moves across a warm air mass, which is forced from the land to the upstream region of Guangdong by the outer circulation of ‘Utor’ while it is approaching Guangdong. The result of the

temperature diagnosis function confirms it. Due to the heating effect of the lower layer, the lower air warms up rapidly and rises, gradually forming a vertical circulation. The vertical circulation causes the convergence of lower-level air towards the center, resulting in a low-level jet stream. One theory suggests that during heavy rainfall processes, the release of latent heat from convective condensation plays an important role in heating the lower atmosphere and contributes to the formation of low-level jet streams [11,12]. The latent heat released by intense precipitation increases available convective potential energy, fostering the development of disturbances. In an unstable atmospheric stratification, the heating from water vapor condensation latent heat leads to mutual promotion between specific wind fields and vertical circulations. This positive feedback process between the two strengthens the horizontal wind field [13], encouraging the formation and development of the low-altitude jet stream. Under the influence of disturbances, the more unstable the atmospheric stratification, the stronger the effect of water vapor condensation heating, resulting in a stronger low-altitude jet stream [14,15].

Previous studies have indicated that condensation latent heat heating plays a significant role in maintaining and evolving low-pressure circulation systems. Diabatic heating in the atmosphere affects the occurrence and development of weather systems and is closely related to weather processes like precipitation [16]. When widespread rainfall occurs in the southern part of East Asia, the corresponding diabatic heating serves as an effective Rossby wave source in the Northwest Pacific, stimulating a wave train that propagates along a great circle path in this region. This diabatic heating process might have a modulating effect on the atmospheric teleconnections in the Northwest Pacific region, potentially influencing weather patterns in East Asia, as well as the development of systems like the Aleutian Low, thereby affecting the distribution of extreme precipitation [17–19]. Scholars have summarized the dynamic and thermodynamic structure of low vortices, noting their significant energy conversion and dispersion characteristics during heavy rainfall processes [20]. Diabatic heating usually leads to the strengthening of cyclones [21]. Precipitation and low vortex occur almost simultaneously, and the release of latent heat from precipitation continuously strengthens the updraft near the center of convection. The enhanced release of condensation latent heat increases the local vorticity, increases the positive vorticity near the center of the low vortex, and enhances the cyclonic circulation [22]. Shen et al. [23] investigated an extratropical cyclone that produced extreme precipitation, calculated the contribution of condensation latent heat release to the relative vorticity tendency of the cyclone, and found that condensation latent heat release can not only directly induce vorticity tendency but also further cause vorticity tendency by changing the temperature gradient. The vorticity occurrence area is always located directly below the center of latent heat heating. Song et al. [24] analyzed through sensitivity experiments and found that the intensity of the low vortex is weak when there is a lack of condensation latent heat heating. The condensation latent heating extends the updraft near the center of the cyclone to the upper levels, resulting in strong convection activities. The deep updraft releases more latent heat, forming a positive feedback mechanism. The positive potential vorticity change generated by the vertical gradient term of condensation latent heating in the lower layer is beneficial to the enhancement of the cyclone [25]. Diabatic heating affects the formation and evolution of clouds in multiple ways. In warm clouds, diabatic heating promotes the formation and growth of water droplets, thereby increasing the intensity and range of precipitation. Precipitation processes dominated by warm clouds are more efficient. In cold clouds, diabatic heating can promote the formation and growth of ice crystals, thereby altering the nature of the clouds and the precipitation process [26,27].

The condensation latent heat released during the heavy rainfall process constitutes the main part of atmospheric diabatic heating. This paper will analyze a regional heavy rainfall process formed by the joint participation of a low-pressure system and a low-level jet stream. By calculating the atmospheric heat source, this paper analyzes its temporal and spatial changes during the heavy rainfall process, revealing the role of diabatic heating in heavy rainfall.

2. Data Sources

This study utilizes daily precipitation data from 124 national ground meteorological observation stations in Shandong province recorded by the China Meteorological Administration. The real-time rainfall data correspond to the hourly precipitation data from these 124 observation stations between 25 and 26 June 2018. The European Centre's ERA5 hourly reanalysis data are used to compute atmospheric heat sources and analyze circulation fields. Satellite cloud images and satellite-observed lightning positioning are sourced from the Fengyun-4 satellite, monitoring data of raindrop spectrum monitors.

The actual formation and dissipation of fronts occur in three-dimensional space. However, in practical analysis and forecasting work, several layers of isobaric charts and surface maps are commonly used to understand the spatial structure of fronts. Therefore, this article will analyze them using the two-dimensional kinematical conditions for frontogenesis. The frontogenesis function is defined as $F = \frac{d|\nabla\theta|}{dt}$, where θ represents the potential temperature [28]. In regions governed by saturated moist air, where condensation precipitation occurs, potential temperature is no longer a conservative quantity. Hence, this study uses equivalent potential temperature, θ_{se} , in lieu of θ . The frontogenesis equation can be rewritten as follows:

$$\frac{d|\nabla\theta_{se}|}{dt} = \frac{\partial|\nabla\theta_{se}|}{\partial t} + u \frac{\partial|\nabla\theta_{se}|}{\partial x} + v \frac{\partial|\nabla\theta_{se}|}{\partial y} \quad (1)$$

Computation of Apparent Heat Source: The “backward method” is employed to calculate the atmospheric apparent heat source [29]. The equation is given as

$$Q_1 = c_p \left[\frac{\partial T}{\partial t} + V \cdot \nabla_P T + \left(\frac{P}{P_0} \right)^{\frac{R}{c_p}} \cdot \omega \frac{\partial \theta}{\partial P} \right] \quad (2)$$

where Q_1 represents the apparent heat source. On the right side of the equation, the terms, respectively, denote local temperature variation, horizontal temperature advection, and vertical temperature variation. Here, T is the temperature, V represents horizontal velocity, ω is the vertical velocity, θ is the potential temperature, and c_p is the specific heat at constant pressure.

Apparent Moisture Sink Calculation: The apparent moisture sink is calculated as

$$Q_2 = -L \left[\frac{\partial q}{\partial t} + \nabla \cdot qV + \frac{\partial q\omega}{\partial p} \right] \quad (3)$$

where Q_2 denotes the apparent moisture sink, and q stands for specific humidity. The term $Q_2 \times c_p$ provides the warming rate induced by the heat released from the condensation of water vapor per unit mass of air over a unit time interval [22]. By vertically integrating Q_1 and Q_2 from the top of the troposphere (taken as 100 hPa) to the ground, we can obtain the overall atmospheric apparent heat sources, $\langle Q_1 \rangle$ and $\langle Q_2 \rangle$.

3. Weather Observations and Meteorological Situation

Affected by the upper-level trough and the shear line at the edge of the subtropical high pressure, Shandong province experienced a widespread heavy rainfall to torrential rain process on 25 June 2018 (Figure 1a). The area of torrential rain was mainly concentrated in the central part of Shandong province, with the maximum rainfall reaching 244.7 mm (in Anqiu, Weifang). This rainstorm event was characterized by its large scale, high magnitude, and intensity. The rainfall in the central part of Shandong province was mainly concentrated from noon to night on the 25th. Among them, Anqiu recorded a maximum 1 h rainfall of 63 mm (Figure 1b), and the provincial capital Jinan recorded an hourly maximum rainfall of 24.1 mm (Figure 1c).

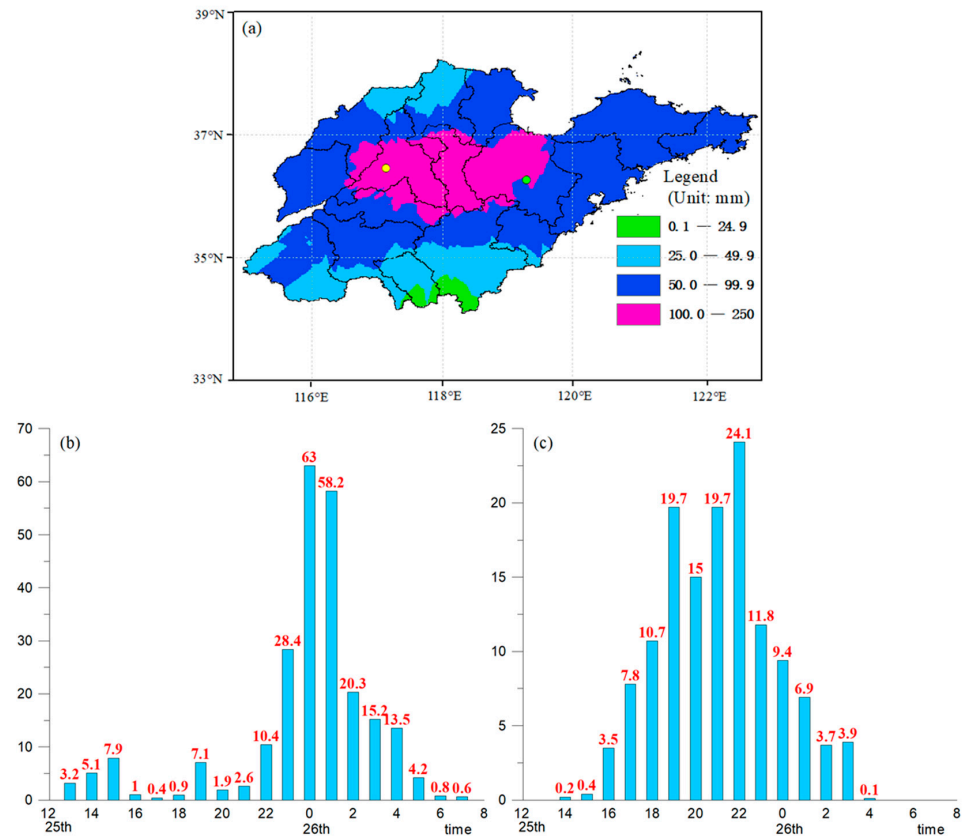


Figure 1. (a) Distribution of precipitation in Shandong province from 08:00 on 25th to 08:00 on 26th (yellow dot: Jinan, green dot: Anqiu); (b) hourly precipitation of Anqiu and (c) Jinan stations.

Figure 2 shows that during the rainfall process, the subtropical high-pressure system and the westerly high-pressure ridge merged and strengthened, stably maintaining along the eastern coast. This acted as a barrier to the upstream low vortex, causing the low vortex system to remain and intensify. From 08:00 to 20:00 on the 25th, the northern trough moved eastward and combined with the southern branch. The 500 hPa subtropical high-pressure system strengthened and extended westward, forming a significant pressure gradient with the low-value system on the west. This led to an increase in the wind speed at the lower 850 hPa layer, intensifying the jet stream. Furthermore, being obstructed by the subtropical high, the trough moved slowly and had a prolonged impact. The central region of Shandong is located on the southern side of the low-level shear line and the left side of the low-level jet stream exit region. The strong low-level convergence and lifting cause water vapor to condense and release unstable energy, forming intense rainfall. A deep and strong southwesterly jet stream is the key system in the formation of this heavy rainfall event. The strong southwest low-level jet stream transports warm and moist air northward, with obvious low-level warming and humidification, enhancing the thermodynamic instability of the stratification. The positive vorticity advection area ahead of the 500 hPa trough intensifies upper-level divergence; the south side of the 850 hPa shear line overlaps with the left side of the southwest jet stream exit area, strengthening low-level convergence. Under this configuration of divergence and convergence, the updrafts strongly develop and are sustained in the central Shandong region, resulting in long-duration, high-efficiency precipitation.

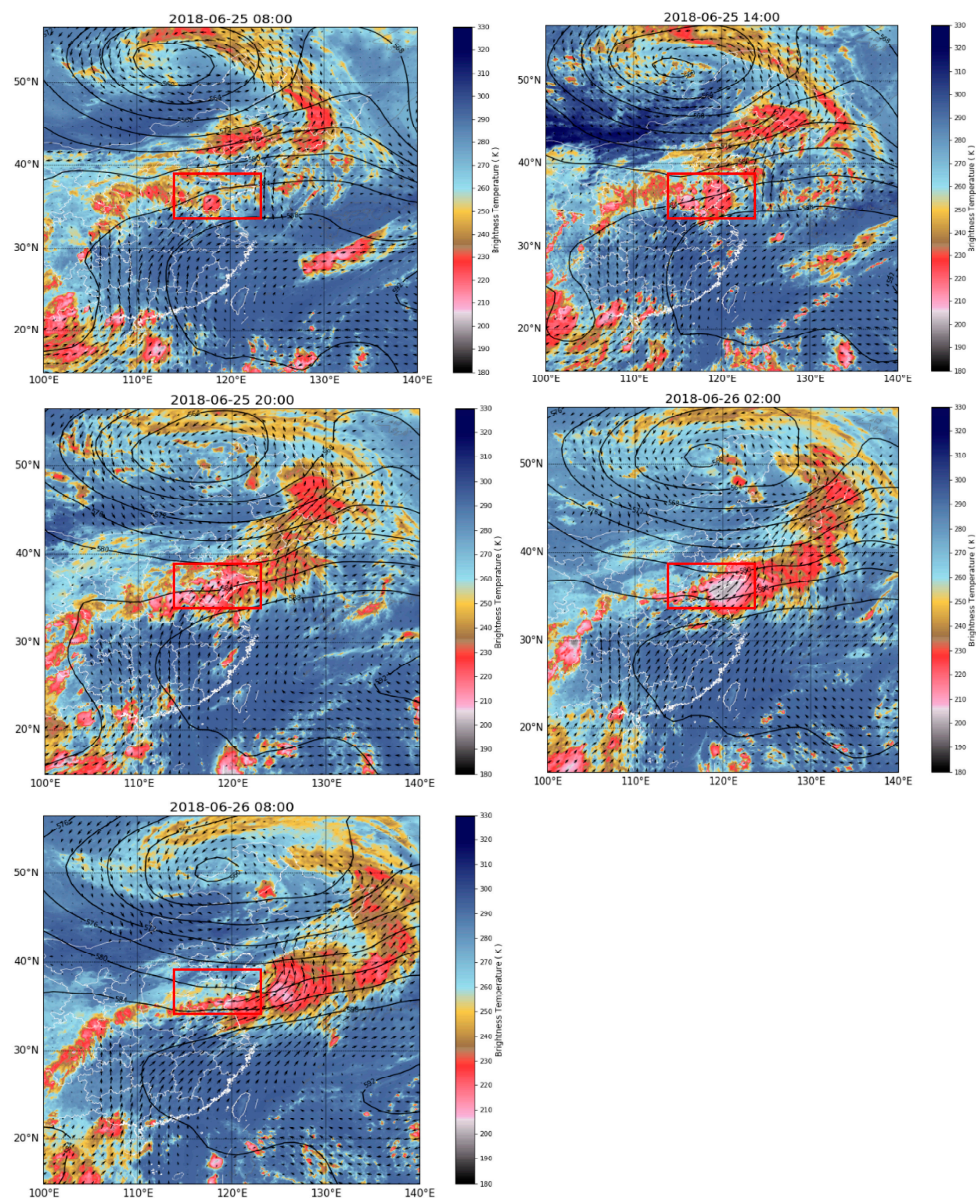


Figure 2. The evolution of 500 hPa height field (isoline, unit: 10 gpm), 850 hPa wind field (vector, unit: $\text{m}\cdot\text{s}^{-1}$), and infrared brightness temperature (shadow) of FY-4 satellite from 08:00 on 25th to 08:00 on 26th (Shandong province is located within the red rectangular box).

From the infrared cloud images (Figure 2), at 08:00 on the 25th, convective cloud clusters gradually developed in the southern part of Shandong province, with the cloud top brightness temperature around 210 K in the most developed areas. By 20:00 on the 25th, the rainfall cloud zone was thriving, and most parts of Shandong province were affected by these rain cloud clusters. By 02:00 on the 26th, as influenced by the low-level jet stream, the rainfall cloud zone moved in a northeast direction and gradually strengthened, with the cloud top brightness temperature of the most active areas around 200 K.

At 08:00 on the 25th (Figure 3a), a moisture channel originating from the South China Sea had already formed. However, most areas of Shandong province were not yet in the convergence zone of moisture flux divergence. By 20:00 on the 25th (Figure 3b), the moisture flux intensified towards the north, and most parts of Shandong province, especially the central region, were in the convergence zone of the moisture flux divergence, resulting in favorable conditions for moisture transportation and accumulation.

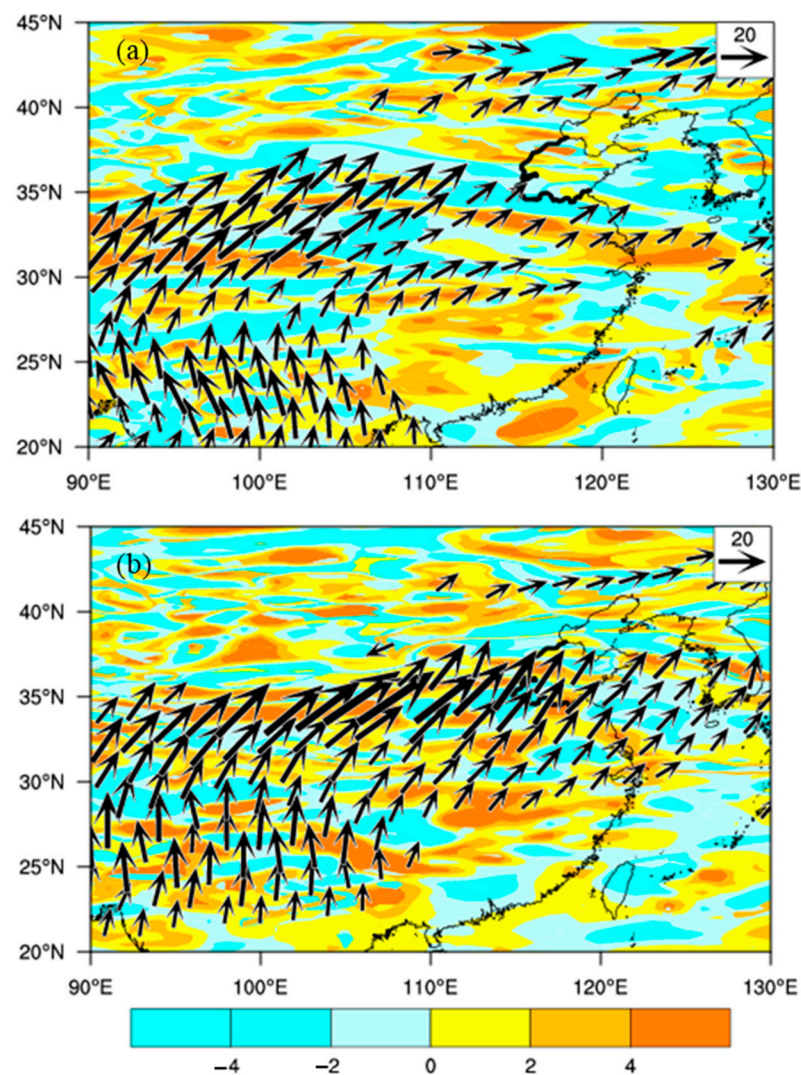


Figure 3. The 850 hPa water vapor flux (vector, unit: $\text{kg}/(\text{m}\cdot\text{s}^{-2})$) and water vapor flux divergence (shadow, unit: $\text{g}\cdot\text{cm}^{-2}\cdot\text{hPa}^{-1}\cdot\text{s}^{-1}$) 08:00 (a) on the 25th and 20:00 (b) on the 25th (the thick solid black line represents the border of Shandong province).

4. Heat Source Analysis

As shown in Figure 1b, the concentrated precipitation period in Anqiu was from 23:00 on the 25th to 02:00 on the 26th. The hourly full-layer wind field and temperature advection in Anqiu from 08:00 on the 25th to 08:00 on the 26th (Figure 4a). At 20:00 on the 25th, the low-altitude jet stream intensified. The low-level jet stream can transport moisture and energy for the precipitation system. However, when the low-level jet stream strengthened, the low-level warm advection did not intensify. Instead, there was a slight increase in cold advection. This is mainly because the rainfall began upstream of Anqiu. Affected by rainfall evaporation, the temperature in the upstream region decreased, which would be slightly lower than in the downstream Anqiu region, making the low-level warm advection not prominent.

At the same time, the concentrated precipitation period in Jinan was from 19:00 to 22:00 on the 25th. The low-altitude jet stream began to strengthen gradually at 17:00, and the low level primarily exhibited cold advection (Figure 4b).

When the low-level jet stream around Anqiu and Jinan intensified, the cold and warm air converged, with both stations located within the front. Figure 5a,b display the horizontal distribution of θ_{se} at 850 hPa at 20:00 on the 25th and 17:00 on the 25th, respectively. There is an east–west oriented dense area of θ_{se} isopleths from the eastern part of Henan to the

northern part of the Shandong province Peninsula. This frontal zone gradually pushed northward. Satellite cloud imagery shows that rain cloud clusters on the southern side of the front, that is, on the side of the warm and moist air, intensified as they moved northward.

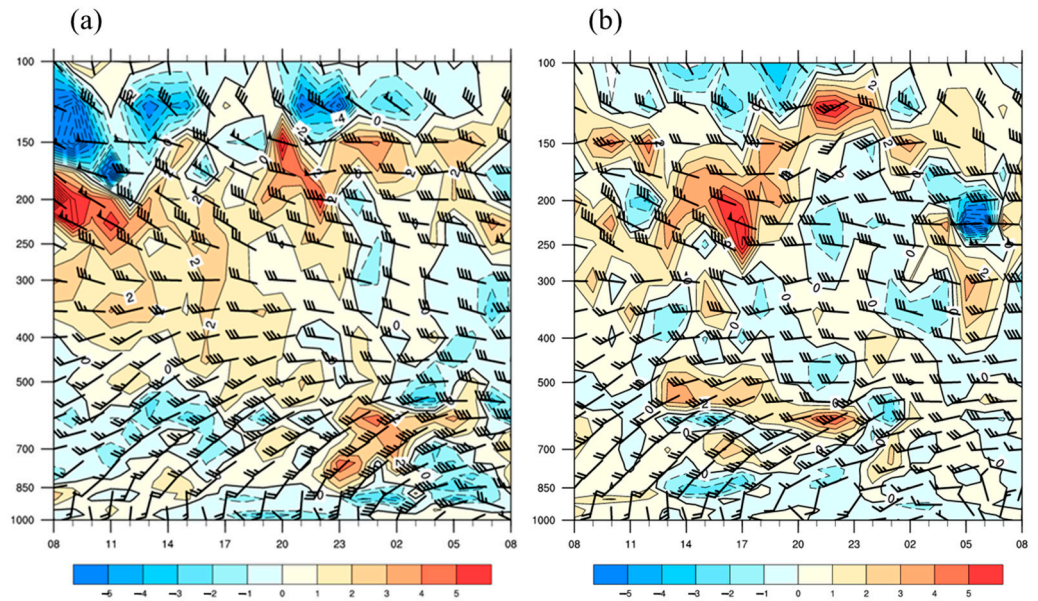


Figure 4. Hourly wind field and temperature advection (unit: °C·km⁻¹) in Jinan (a) and Anqiu (b) from 08:00 on 25th to 08:00 on 26th.

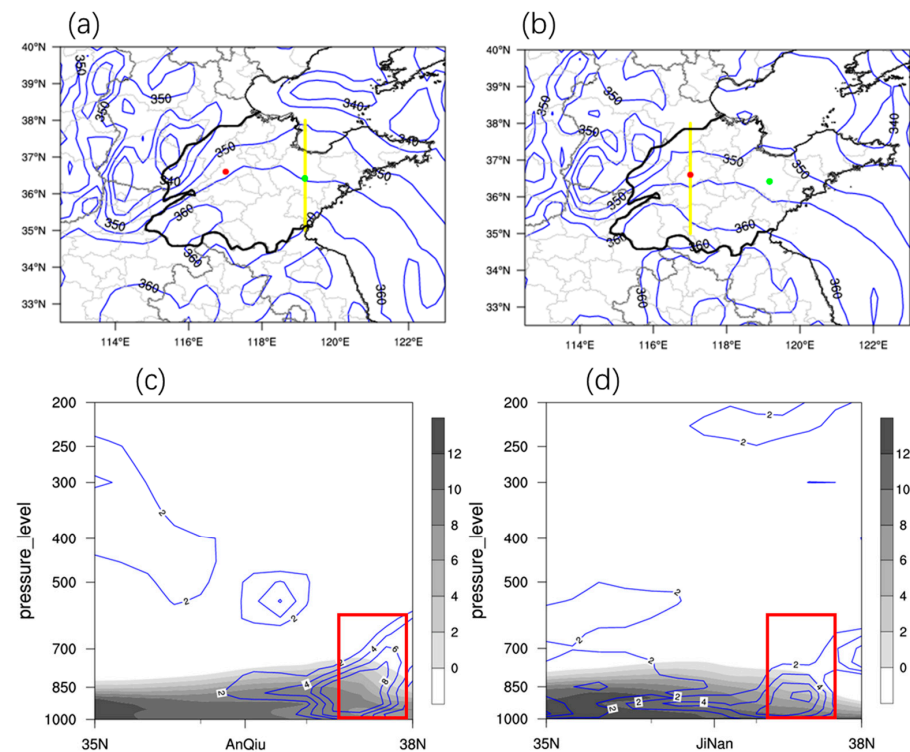


Figure 5. Schemes from 20:00 on 25th (a) and 17:00 on 25th (b) θ_{se} (unit: K, red dot: Jinan, green dot: Anqiu). Vertical profiles of specific humidity (shadow, unit: g/kg) and two-dimensional kinematic frontogenesis function value (contour, unit: $10^{-10} \text{ K} \cdot \text{m}^{-1} \cdot \text{s}^{-1}$) at 20:00 on the 25th (c) and 17:00 on the 25th (d) (Figure (c) is the profile along the yellow solid line in Figure (a), and Figure (d) is the profile along the yellow solid line in Figure (b), the red rectangular indicates the frontogenesis area).

Vertical cross-sections along the front (Figure 5c,d) indicate that with the strengthening of the low-altitude jet stream, there is kinematic frontogenesis near Anqiu and Jinan below 700 hPa, with the maximum values exceeding $8 \times 10^{-10} \text{ K} \cdot \text{m}^{-1} \cdot \text{s}^{-1}$. As the low-altitude jet stream intensified, there was a slight increase in cold advection near Anqiu and Jinan. The convergence of cold and warm air at both stations was not pronounced, with a small temperature gradient. The vertical distribution of humidity (Figure 5c,d) indicates a large humidity gradient within the front. It can be seen that in this process, the low-level jet stream transported moisture, enhancing the humidity gradient and strengthening the kinematic frontogenesis.

The FY-4 satellite lightning location monitoring detected lightning at 13:15:10 and 17:25:10 on the 25th near Anqiu and Jinan, respectively. Simultaneously, radar echoes showed that both areas generated echoes above 40 dBZ before and after the appearance of lightning (Figure 6). Prior to the onset of this convection, the mid and lower layers of the atmosphere over Anqiu and Jinan were dominated by cold advection. The energy sources before these two convective events were not primarily from the warm advection delivered by the low-altitude jet stream. Instead, local thermal conditions provided the energy source, allowing the unstable atmospheric stratification to continuously develop.

To further verify this point, the impact of three components influencing the atmospheric heat source was calculated through atmospheric heat source analysis. Since the magnitude of the vertical temperature variation is relatively small, only the local temperature variation and horizontal advection of the atmospheric heat source between 08:00 on the 25th and 14:00 on the 26th for both Anqiu and Jinan were analyzed (Figure 7a,b). The comparison revealed that the horizontal advection of temperature at both stations during and prior to the concentrated rainfall period was less than the local temperature variation. Thus, during the period of concentrated rainfall, the thermal conditions were maintained and developed, with local temperature changes being the primary contributor.

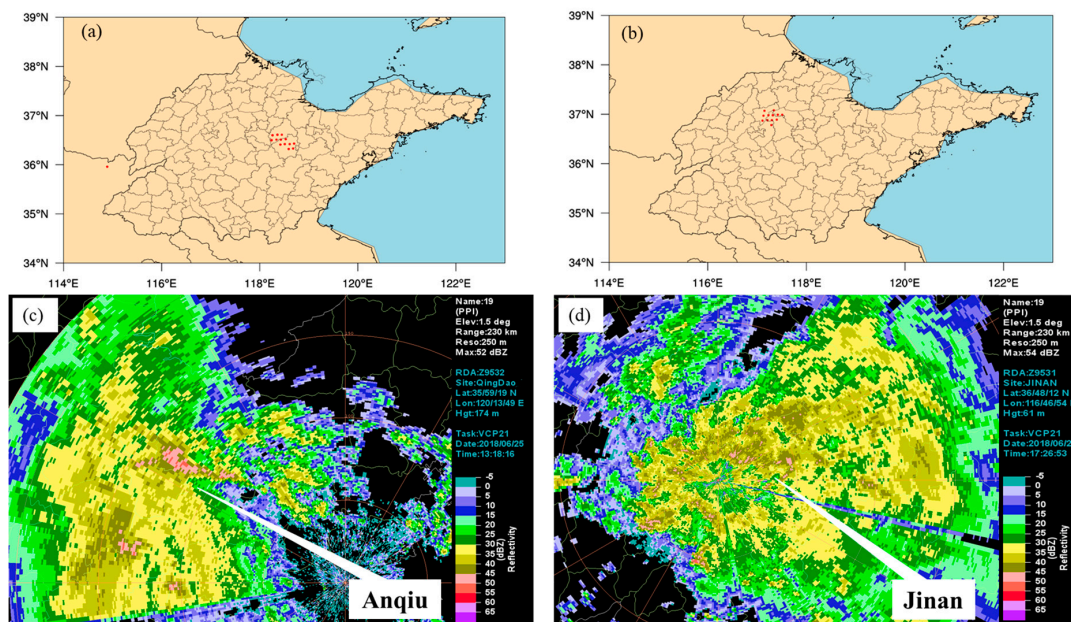


Figure 6. Lightning location of FY-4 satellite at (a) 13:15:10 on 25th and (b) 17:25:10 on 25th; (c) 13:18:16 on the 25th and (d) 17:26:53 on the 25th, 1.5 degree radar basic reflectivity (in Figure (a) and (b), the red dots indicate the locations where lightning has been detected).

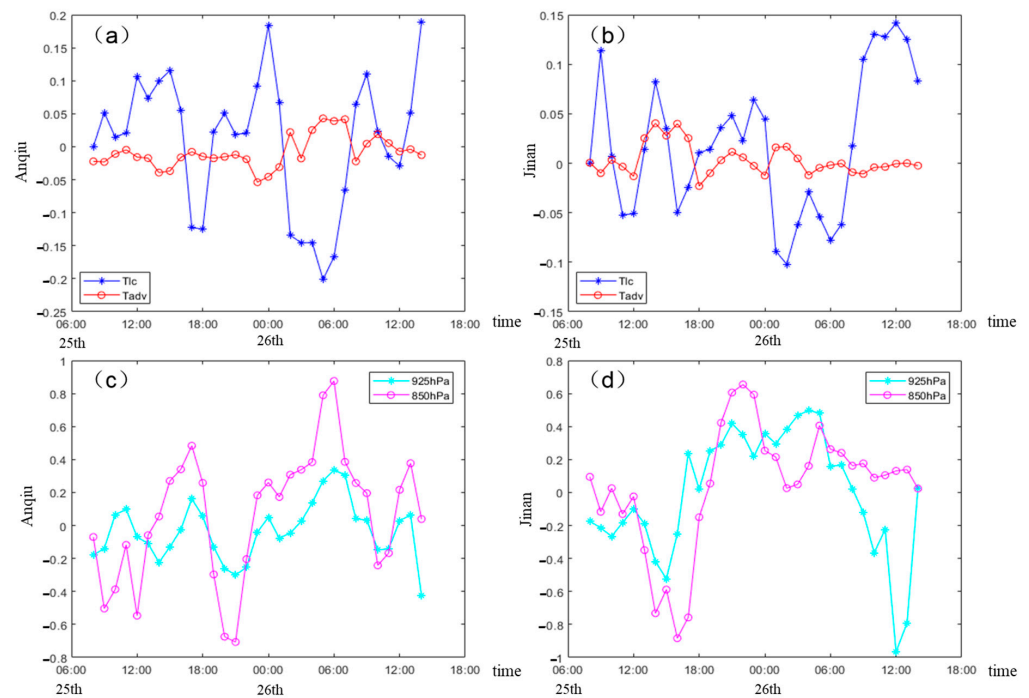


Figure 7. Local variation in atmospheric heat source temperature (blue) in Anqiu (a) and Jinan (b) from 08:00 on 25th to 14:00 on 26th and horizontal advection term (red) of atmospheric heat source temperature (unit: Wm^{-2}); 925 hPa (cyan) and 850 hPa (pink) warming rate caused by heat released from water vapor condensation (unit: $\text{K}\cdot\text{h}^{-1}$) in Anqiu (c) and Jinan (d).

During periods of intense rainfall, the latent heat released from moisture condensation will have a localized heating effect on the atmosphere, which can influence the intensity of the weather system. By calculating the warming rate caused by the latent heat released from moisture condensation per unit time and per unit mass of air for both Anqiu and Jinan from 08:00 on the 25th to 14:00 on the 26th (Figure 7c,d), it was observed that there was a significant increase in the warming rate for both stations during and prior to the period of concentrated rainfall. The latent heat released during the intense rainfall period resulted in a net heating of the atmosphere.

Raindrop spectrum monitors in the Anqiu area from 23:01 to 24:00 on the 25th and in the Jinan area from 21:01 to 22:00 (the time of the maximum one-hour rainfall) showed that raindrop diameters were mainly concentrated below 2 mm. The particle number distribution of the raindrop spectrometer indicated a higher concentration of small droplets in this precipitation process, with particle descent speeds generally below 15 m/s, especially those below 10 m/s (Figure 8). The convective storm development height of the precipitation was low, and the hourly rainfall was particularly intense, showing typical characteristics of short-duration intense precipitation in warm clouds. During the time of the maximum one-hour rainfall in Anqiu and Jinan, the positive feedback of condensation latent heat was more evident, leading to the formation and growth of small droplets in warm clouds, thus increasing the intensity of the precipitation.

From an overall perspective of the entire atmospheric layer, at the time of Anqiu's maximum hourly precipitation at 0:00 on the 26th, there was an enhanced warming rate caused by the release of heat from water vapor condensation between 1000 and 250 hPa. Two major value centers were located above 500 hPa and between 850 and 700 hPa (Figure 9a). During the precipitation process, evaporation causes cloud layers to develop upward. As a result, there is a center of maximum warming rate above 500 hPa during the peak rainfall period. The increase in temperature rate at 850–700 hPa begins earlier. Due to the enhancement of the low-level jet stream (Figure 2), the water vapor advection is enhanced. According to Formula (3), the temperature rate will increase accordingly. That is, the strengthening of

the low-level jet stream and the increase in water vapor advection will heat the mid-lower layers during the period of intense rainfall, which will also lead to the further strengthening of the low-level jet stream. At the same time, the vorticity value increases, the cyclonic circulation strengthens, and the lower layer is a negative divergence center, strengthening the convergence of the lower layer (Figure 9c). At 22:00 on the 25th, when Jinan experienced its maximum hourly precipitation, there was also an enhanced warming rate caused by the release of heat from water vapor condensation (Figure 9b). Simultaneously, vorticity values increased, and the upper-level trough and shear systems strengthened. The lower layers exhibited a divergence negative value center, while the mid and upper layers had a divergence positive value center, forming an upper divergence and lower convergence situation (Figure 9d). This intensified the cyclonic circulation system and upward motion in the lower layers. This indicates that during the period of intense rainfall, the feedback from the release of latent heat from moisture condensation strengthens the atmospheric system, providing powerful thermodynamic and dynamic conditions for intense rainfall.

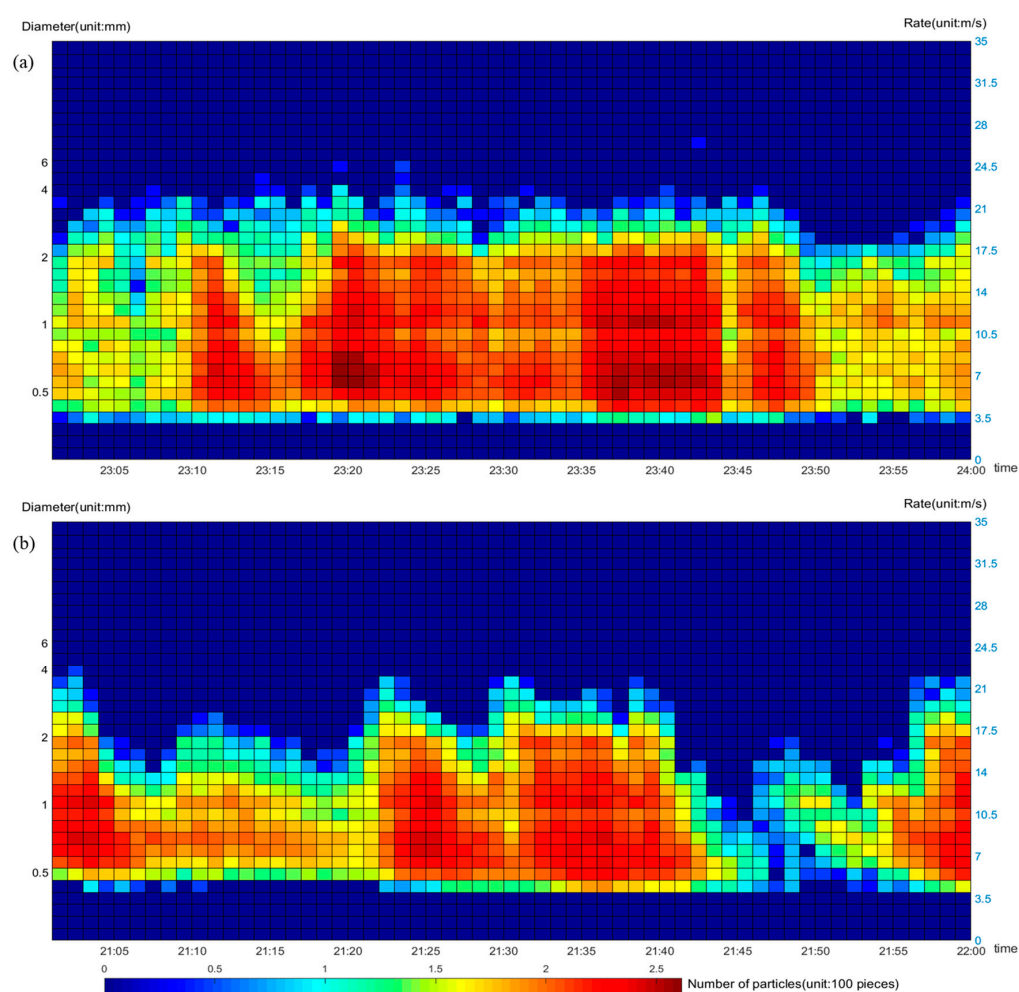


Figure 8. The monitoring data of the raindrop spectrum monitors in Anqiu from 23:01 to 24:00 on the 25th (a) and in Jinan from 21:01 to 22:00 on the 25th (b) (left Y axis is the diameter of raindrop particles, unit: mm; right Y axis is the falling speed of raindrop particles, unit: m/s; color scale is the number of particles, unit: 100 pieces).

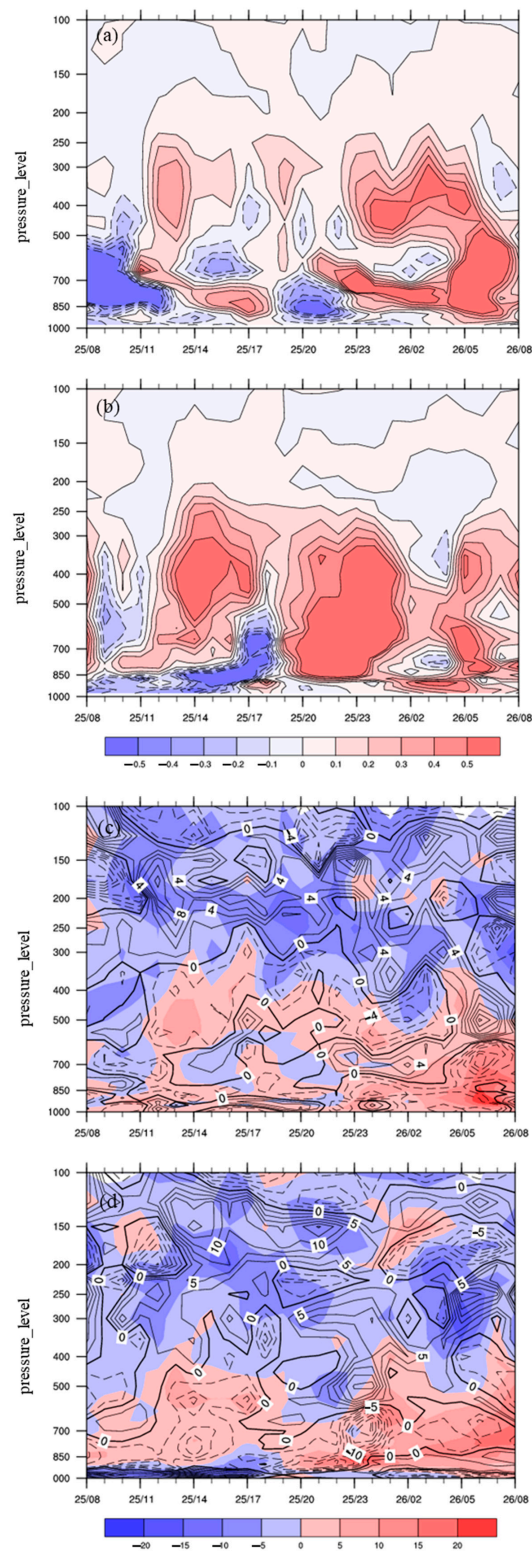


Figure 9. Hourly temperature increase rate caused by heat released in water vapor condensation in Anqiu (a) and Jinan (b) from 08:00 on 25th to 08:00 on 26th (unit: $\text{K}\cdot\text{h}^{-1}$); vorticity (shadow, unit: 10^{-5}s^{-1}) and divergence (isoline, unit: 10^{-5}s^{-1}) in Anqiu (c) and Jinan (d).

5. Conclusions and Discussions

This study focused on the widespread heavy to torrential rain process in Shandong province on 25 June 2018. The concentrated rainfall area was in central Shandong province.

A deep and robust southwesterly jet stream was identified as the key system behind this rain event. During the period of concentrated rainfall and the intensification of the low-altitude jet stream, the overlying atmosphere at the observation stations was dominated by cold advection. This was primarily because rainfall commenced upstream, and as a result of the rainfall, temperatures in the upstream areas dropped, being slightly cooler than downstream areas. From this, it is evident that in this process, the warm advection in the low-altitude jet stream was not the primary energy supplier for the heavy rainfall. The jet stream transported moisture, increased humidity gradients, and intensified frontogenesis. When comparing local temperature variations with horizontal temperature advection, it was observed that the latter was often less significant than the former during and before the concentrated rainfall. Therefore, during the concentrated rainfall period, the evolution of local temperature and thermal conditions, as well as their configuration with the low-level jet, was crucial. The strengthening of the low-level jet stream leads to an increase in water vapor advection, and the increase in the rate of temperature increase caused by the condensation of water vapor in the lower layers releases heat. The warming in the lower layers increases the effective potential energy, promoting the development of disturbances. Under the influence of the disturbance field, the more unstable the atmospheric stratification, the stronger the heating effect of water vapor condensation, and the stronger the intensity of the low-level jet stream formed. Precipitation processes dominated by warm cloud rainfall are highly efficient. Raindrop spectrometer data showed that during the maximum one-hour rainfall in Anqiu and Jinan, the positive feedback of condensation latent heat was quite evident, leading to the formation and growth of small droplets in warm clouds, thereby increasing the intensity of the precipitation. The latent heat release from water vapor condensation led to the development of the wind field and vertical circulation. During and before the concentrated rainfall period, the heating rate caused by the latent heat release in unit mass air over unit time showed a notable increase. The enhanced heating rate due to latent heat release played a warming role in the middle and lower atmosphere during the concentrated rainfall period. The positive feedback from the latent heat release amplified the weather system, affecting the rainfall and providing robust thermal and dynamical conditions for heavy rainfall.

In the study of diabatic heating, data are a key issue. The continuous and stable operation of the newly launched next-generation geostationary orbit quantitative remote sensing meteorological satellites will provide us with higher-quality satellite remote sensing data. It will aid in further research related to diabatic heating. The occurrence of a precipitation process is mainly influenced by the combined effects of various weather systems at different altitudes. Changes in the location and intensity of these weather systems inevitably affect the location, intensity, and duration of precipitation. Since diabatic heating is an important factor influencing weather systems, the precipitation process caused by these systems is inextricably linked to diabatic heating. Weather systems, as the link between precipitation occurrence and the release of condensation latent heat, require further study regarding how their strength and position are affected by diabatic heating processes. Numerical modeling is the current trend, as it includes various diabatic parameterization schemes. Improving and comprehensively detailing these diabatic processes will undoubtedly aid in understanding diabatic processes and their effects. However, how to better integrate diabatic heating into meso- and small-scale numerical weather prediction models is a topic worthy of further exploration. Additionally, how the impact of diabatic heating processes on weather systems and rainfall can be applied in numerical model corrections requires more case studies and numerical experiments for realization and is worth further research and discussion.

Regarding the feedback effects of diabatic heating on weather systems and precipitation, current research achievements have only reached preliminary qualitative conclusions, and more practically significant quantitative relationships have yet to be clarified. Most studies have used composite analysis methods and only summarized the general impact of diabatic heating on the location and intensity of precipitation without providing a quanti-

tative impact on rainfall intensity. Additionally, how diabatic heating near weather-scale systems specifically affects the detailed process of a precipitation event is also worth further study. The precipitation process analyzed in this paper occurred on the edge of the Western Pacific Subtropical High, a major planetary-scale weather system affecting the distribution of rainbands in East Asia. The classical theory once believed that the subtropical high is caused by lower-level divergence under meridional circulation sinking in the subtropical region. However, extensive research by meteorologists has shown that the formation and changes in the subtropical high are the comprehensive results of atmospheric motion subject to internal and external forcing [30]. Scholars have theoretically and through simulations proved that Earth's rotation and diabatic heating are the main reasons for the formation of the summer subtropical high and found that the release of condensation latent heat is a key factor determining the position and strength of the summer subtropical high in the Eastern Hemisphere [31,32]. Therefore, further analysis is needed on the short-term variations in the position of the subtropical high and its connection to the field of diabatic heating.

In this heavy rainfall weather process, forecasters failed to predict the torrential rain in the central and northern regions of Shandong province, as they often did not consider the strengthening of the weather system over time due to the impact of high and low altitude jet stream coupling and condensation latent heat heating, and the potential conditional symmetric instability, leading to cognitive biases and the missed forecast of the heavy rain. For such warm-region heavy rainfall processes, forecasters should consider the trajectory of the Western Pacific Subtropical High, the coupling of high and low altitude jet streams, the impact of condensation latent heat release on the low-level jet stream and southerly winds, and the potential mechanism of conditional symmetric instability. By integrating numerical models and appropriately adjusting the predicted rainfall amount in the models, the possibility of heavy rainfall can be comprehensively considered.

Author Contributions: Y.J.: Conceptualization, Writing—Original Draft, Resources, Formal analysis, Validation; M.Z.: Writing—Review & Editing, Data Curation; Y.Z.: Investigation, Methodology, Funding acquisition, Project administration; Y.C.: Investigation. All authors have read and agreed to the published version of the manuscript.

Funding: This study is supported by the Key Project of China Meteorological Administration (2023ZDIANXM03), Shandong Provincial Meteorological Bureau Guidance Project (2021SDYD22), and Shandong Provincial Natural Science Foundation General Project (ZR2021MD012).

Institutional Review Board Statement: Not applicable.

Informed Consent Statement: Not applicable.

Data Availability Statement: Data available on request due to restrictions eg privacy or ethical. The data presented in this study are available on request from the corresponding author. The data are not publicly available due to a confidentiality agreement with China Meteorological Administration.

Acknowledgments: We are very grateful to the reviewers for their constructive comments and suggestions.

Conflicts of Interest: The authors declare no conflict of interest.

References

1. Zhou, X.S.; Wu, W.; Sun, X.C. Statistical characteristic analysis of weather forecast indicators for heavy rainfall in Shandong. *Meteorology* **2014**, *40*, 744–753. (In Chinese)
2. Shi, X.M.; Wang, Z.X.; Sun, J.L.; Sun, J.L.; Gu, Y. Spatial and temporal distribution and circulation characteristics analysis of extreme summer precipitation in Shandong. *Bull. Oceanogr. Limnol.* **2020**, *2020*, 45–51. (In Chinese)
3. Diao, X.G.; Liu, C.; Wan, M.B.; Hou, S.M. Analysis of cloud street radar echo characteristics and their effects during three severe rainstorm events in Shandong. *Meteorology* **2020**, *46*, 179–188. (In Chinese)
4. Lu, W.X.; Ye, Z.X.; Zhuang, Q.B.; Yu, Z.S. Comparative analysis of two heavy rainfall events affected by low-level southeast wind jet. *Torrential Rain Disasters* **2011**, *30*, 227–233. (In Chinese)
5. Lu, H.Z.; Sun, X.L.; Liu, Y.W.; Sun, J.Y. Development characteristics of mesoscale convective systems in a scattered heavy rain event. *J. Arid. Meteorol.* **2018**, *36*, 667–675. (In Chinese)

6. Zhang, Q.; Su, L.L.; Zhang, X.Z.; Yuan, J.; Zhou, S.H. Environmental characteristics and triggering mechanism of a warm-sector heavy rain event in Shandong. *J. Arid. Meteorol.* **2019**, *37*, 933–943. (In Chinese)
7. Zhu, Q.G.; Zhou, W.C.; Zhang, H.X. Mechanism of high and low-level jet coupling in the formation of the Yangtze River middle reaches rainstorm. *J. Nanjing Inst. Meteorol.* **2001**, *24*, 308–314. (In Chinese)
8. Liang, S.J.; Ma, X.H. Comparative analysis of two typical heavy rain events in the eastern part of Northwest China. *Meteorol. Mon.* **2012**, *38*, 804–813. (In Chinese)
9. Huang, X.Y.; Sun, J.S.; Liu, W.T. Evolution of low-level jet under terrain influence and its interaction with intense precipitation convective storm system. *Acta Meteorol. Sin.* **2020**, *78*, 551–567. (In Chinese)
10. Cheng, Z.Q.; Lin, L.X.; Sha, T.Y.; Yang, G.J. Thermal conditions analysis of the “Yout” extreme rainstorm process. *Meteorol. Mon.* **2014**, *40*, 1507–1512. (In Chinese)
11. Xu, W.J.; Liu, C. A mechanism for the formation of low-level jet and its numerical simulation experiment. *J. Nanjing Inst. Meteorol.* **1985**, *8*, 231–239. (In Chinese)
12. Tao, W.K.; Li, X.W. The relationship between latent heating, vertical velocity, and precipitation processes: The impact of aerosols on precipitation in organized deep convective systems. *J. Geophys. Res. Atmos.* **2016**, *121*, 6299–6320. [[CrossRef](#)]
13. Jiang, D.C.; Wei, T.J. Energetics analysis of the Southwest low-level jet. *J. Nanjing Inst. Meteorol.* **1983**, *2*, 204–214. (In Chinese)
14. Fu, J.; Ma, X.K.; Chen, T.; Zhang, F.; Zhang, X.D.; Sun, J.; Quan, W.Q.; Yang, S.N.; Shen, X.L. Characteristics and Synoptic Mechanism of the July 2016 Extreme Precipitation Event in North China. *Meteorol. Mon.* **2017**, *43*, 528–539. (In Chinese)
15. Brian, J.C.; Belay, B.D.; Ruben, D. An overview of low-level jet winds and corresponding mixed layer depths during PECAN. *J. Geophys. Res. Atmos.* **2019**, *124*, 9141–9160. [[CrossRef](#)]
16. Yao, X.P.; Yan, L.Z.; Zhang, S. Research progress and prospect of atmospheric non-adiabatic heating effects. *Meteorol. Mon.* **2019**, *45*, 1–16. (In Chinese)
17. An, X.; Sheng, L.; Liu, Q.; Li, C.; Gao, Y.; Li, J. The combined effect of two westerly jet waveguides on heavy haze in the North China Plain in November and December 2015. *Atmos. Chem. Phys.* **2020**, *20*, 4667–4680. [[CrossRef](#)]
18. An, X.; Sheng, L.; Li, C.; Chen, W.; Tang, Y.; Huang, F.J. Effect of rainfall-induced diabatic heating over southern China on the formation of wintertime haze on the North China Plain. *Atmos. Chem. Phys.* **2022**, *22*, 725–738. [[CrossRef](#)]
19. An, X.; Chen, W.; Li, C.; Cheng, L.; Zhang, W.; Hai, S.; Hu, P. Influence of rainfall-induced diabatic heating on southern rainfall-northern haze over eastern China in early February 2023. *Sci. China Earth Sci.* **2023**, *66*, 2579–2593. (In Chinese) [[CrossRef](#)]
20. Yao, J.; Zeng, Y.; Li, J.; Yang, L. A Review of Dry-Wet Climate Change and Extreme Precipitation in Central Asia. *Adv. Meteorol. Sci. Technol.* **2020**, *10*, 7–14. (In Chinese)
21. Zhang, S.Q.; Xu, J.J.; Ji, J.G.; Tang, R.Y.; Long, J.C. Development mechanism of a strong explosive cyclone over the northeastern Pacific. *J. Meteorol. Sci.* **2021**, *41*, 349–362. (In Chinese)
22. Chen, P.; Liu, D.; Pang, Y.; He, J.; Zhou, Y.Y. Diagnosing the vortex budget and latent heat release during the development of a southwest vortex. *J. Arid. Meteorol.* **2015**, *33*, 934–940. (In Chinese)
23. Shen, Y.; Sun, Y.; Liu, D. Effect of condensation latent heat release on the relative vorticity tendency in extratropical cyclones: A case study. *Atmos. Ocean. Sci. Lett.* **2020**, *13*, 275–285. [[CrossRef](#)]
24. Song, W.; Li, G.; Tang, Q. Numerical experiments on the influence of heating and water vapor on two plateau vortices. *Chin. J. Atmos. Sci.* **2012**, *36*, 117–129. (In Chinese)
25. Xu, W.J.; Zhang, Y.C. Numerical study on the feedback between latent heating and convection in a Qinghai-Tibetan Plateau vortex. *Plateau Meteorol.* **2017**, *36*, 763–775. (In Chinese)
26. Madhulatha, A.; Dudhia, J.; Park, R.S.; Bhan, S.C.; Mohapatra, M. Effect of Single and Double Moment Microphysics Schemes and Change in Cloud Condensation Nuclei, Latent Heating Rate Structure Associated with Severe Convective System over Korean Peninsula. *Atmosphere* **2023**, *14*, 1680. [[CrossRef](#)]
27. Xu, J.; Ping, F.; Li, J.Y.; Du, H. A study of cloud microphysical processes and a mesoscale environment in a heavy rainfall case over Yan’an. *Front. Earth Sci.* **2023**, *11*, 1149856. [[CrossRef](#)]
28. Wu, R. *Principles of Modern Meteorology*; Higher Education Press: Beijing, China, 1999. (In Chinese)
29. Yanai, M.; Li, C.F.; Song, Z.S. Seasonal heating of the Tibetan Plateau and its effects on the evolution of the Asian summer monsoon. *J. Meteorol. Soc. Jpn.* **1992**, *79*, 419–434.
30. Liu, Y.M.; Wu, G.X. Review of the Subtropical High Research and Reconsideration of Several Fundamental Issues. *Acta Meteorol. Sin.* **2000**, *58*, 500–512. (In Chinese)
31. Rodwell, M.J.; Hoskins, B.J. Monsoons and the dynamics of deserts. *Q. J. R. Meteorol. Soc.* **1996**, *122*, 1385–1404. [[CrossRef](#)]
32. Wang, L.J.; Gao, H.; Guan, Z.Y.; He, J.H. Relationship between the western Pacific subtropical high and the subtropical East Asian diabatic heating during south China heavy rains in June 2005. *J. Meteorol. Res.* **2011**, *25*, 203–210. [[CrossRef](#)]

Disclaimer/Publisher’s Note: The statements, opinions and data contained in all publications are solely those of the individual author(s) and contributor(s) and not of MDPI and/or the editor(s). MDPI and/or the editor(s) disclaim responsibility for any injury to people or property resulting from any ideas, methods, instructions or products referred to in the content.